REPORT 895-2

RADIO PROPAGATION AND CIRCUIT PERFORMANCE AT FREQUENCIES BELOW ABOUT 30 kHz

(Study Programme 31D/6)

(1982-1986-1990)

1. Introduction

Because of the stability of propagation (amplitude and phase), frequencies in the VLF range are used for standard frequency and time broadcasts [Blair *et al.*, 1967] and a wide range of communications and navigational applications [Casselman *et al.*, 1959]. In particular, it has been found that the stability of transmission permits frequency comparison to within a few parts in 10^{12}, which is four orders of magnitude better than is possible at HF, thus permitting long-range navigation utilizing phase comparison between spaced atomic frequency-controlled or phase-locked transmissons. Navigation and location accuracies of 1 to 3 nautical miles are achieved by the Omega navigation system [Beukers, 1974]. Accuracies of an order of magnitude better than this have been obtained utilizing a differential Omega technique, in which a fixed station is utilized to establish reference corrections for diurnal and disturbance variations for a nearby mobile station [Nard, 1972; Beukers, 1973].

The ELF band (30-3000 Hz) has very serious deficiencies when compared with conventional radio communications bands. Its restricted bandwidth implies very low data rates, and because of the very large wavelength, whatever transmitting antenna could be built would be inefficient, as measured by radiated power [Burrows, 1978]. For specific applications, however, where part of the propagation path involves lossy media such as rock, earth, soil and water, ELF offers the possibility of communicating whereas conventional bands offer none. Even at VLF (3 to 30 kHz) where the wavelength is one to two orders of magnitude smaller, efficient transmitting antennas must be enormous costly structures, and transmitting powers great if global communications are desired, particularly to points under the sea and beneath the ground.

ELF transmissions are useful for global communications and for communications to points under the sea or beneath the ground [Burrows and Nielssen, 1972; Willim, 1974]. Due to the technical difficulties of radiating energy in the ELF band at high enough power to be detected at thousands-of-kilometre ranges, very little data have been gathered until quite recently. Kuhnle and Smith [1964] measured attenuation rates of a 400 Hz continuous wave signal and Davis [1976] and Bannister [1979] have measured attenuation rates as well as relative phase for ELF waves in the 40 to 50 and 70 to 82 Hz frequency bands. ELF atmospherics have been observed since 1966 [Taylor and Sao, 1970; Hughes and Theissen, 1970; Hughes, 1971; Chapman *et al.*, 1966]. A detail-

quantitative description of these data is difficult because, on the one hand, the complex wave number depends upon the lower ionosphere structure, which is not uniform in position, time or direction, and on the other hand, because propagation measurements depend on naturally-occurring lightning strokes (sferics) as a signal source. One experiment was conducted to evaluate the averaging of propagation parameters of ELF waves propagating over a path in which the ionospheric environment changed within one wavelength [Hughes and Gallenberger, 1974].

Several methods (with corresponding computer programs) have been developed for calculating signal levels at ELF. Among these are those described by Johler and Lewis [1969]; Lewis and Johler [1976]; and Pappert and Moler [1974]. Barr [1971a and 1971b] has given especially complete numerical results of propagation parameters in the frequency range from 1 to 10 kHz. An extensive summary of ELF communications theory and measurement is available in Galejs [1972] and Wait [1974 and 1977].

The mode theory, which is used extensively at VLF and may be used efficiently at LF up to at least 60 kHz, is a full wave theory that includes diffraction and surface wave propagation. The waves are considered to propagate between the Earth and the ionosphere as normal modes, analogous to microwave propagation in a lossy wave-guide [Al'pert *et al.*, 1967; Budden, 1961; Galejs, 1967a and 1967b; Pappert, 1968; Volland, 1966; Wait, 1962 and 1964]. For frequencies above about 30 kHz the wave-guide is many wavelengths high, for short distances many propagating modes must be considered, but at VLF and distances greater than 1000 km only a few modes need be considered. While the physical picture of wave-guide mode theory is less easy to visualize compared with ray-paths it provides a better explanation of certain features of VLF propagation which are not readily explicable on ray-path/wave-hop theory.

VLF and LF transmitters in common use radiate a vertically polarized field. Although the ionosphere and terrestrial magnetic field may, in principle, introduce a horizontally polarized component, there is no experimental evidence which demonstrates that such fields are significant at great distances. Theoretical calculations [Snyder and Pappert, 1969; Foley *et al.*, 1973] suggest, however, that at night in low latitudes there may be considerable horizontal polarization.

Horizontal electric dipole excitation of vertical E field at the ground for 19.8 kHz radiation beneath a hypothetical daytime ionosphere and beneath a highly anisotropic ionosphere has been numerically investigated as a function of ground conductivity and source elevation [Pappert, 1970]. Results show that for source elevations comparable to or greater than a wavelength, horizontal and vertical electric dipole excitations can become comparable. Also, when one end or both ends of a propagation path are at an elevated position, gains in signal amplitude can be achieved by using transmitting and receiving antenna orientations other than vertical [Pappert and Bickel, 1970]. This property is of particular importance for air-to-air VLF and LF communications.

2. Calculating field strength by waveguide mode methods: early approaches

2.1 *Calculating field strength in a spherical homgeneous guide*

The field strength, E, from a transmitter at a distance d km, on the ground, can be calculated by [Wait, 1962]:

$$E = \frac{300\sqrt{p}}{\sqrt{a \sin d/a}} \cdot \frac{\sqrt{\lambda}}{h} e^{-i(kd+\pi/4)} \sum_n \Lambda_n e^{-ikS_n d} \quad \text{mV/m} \qquad (1)$$

where

p: radiated power (kW),

a: radius of the Earth (km),

λ: free space wavelength (km),

k: $2\pi/\lambda$,

Λ_n: excitation factor for the nth mode,

kS_n: propagation constant,

d: path distance (km),

h: height of ionosphere (70 km-day; 90 km-night).

In general, the terms Λ_n and S_n are complex. The excitation factor Λ_n gives the relative amplitude and phase of each mode of order n excited in the Earth-ionosphere wave-guide by the source. The real part of the propagation constant kS_n contains the phase information for each mode while the imaginary part determines the attenuation rate. In order to obtain the field strength the contributions of each mode must be summed giving proper attention to the relative phases of the terms. Modification is required near the antipode when $d/a \approx \pi$.

The field strength for mode n is:

$$E_n = \frac{300\sqrt{p}}{\sqrt{a \sin d/a}} \cdot \frac{\sqrt{\lambda}}{h} \mid \Lambda_n \mid e^{-\alpha_n d} e^{i(\Phi_n - kd \operatorname{Re} S_n)} \quad \text{mV/m} \tag{2}$$

where:

$$\Lambda_n \text{ (excitation factor)} = \mid \Lambda_n \mid e^{i\Phi_n}$$

$$\alpha_n \text{ (attenuation factor)} = \frac{2\pi}{\lambda} \operatorname{Im} S_n$$

$$= -8.68 \cdot \frac{2\pi}{\lambda} \operatorname{Im} S_n \quad \text{dB/km}$$

$\operatorname{Im} S_n$ and $\operatorname{Re} S_n$ denote the imaginary and real parts of S_n respectively. The phase velocity $V_n = c/\operatorname{Re} S_n$, where c is the free space velocity.

In most cases, it is practical to derive field strength versus distance curves [Watt, 1967]. The recommended method is to start with appropriate values of Λ_n and S_n and perform the calculations in equation (1). Where more than one mode is present, it is necessary to interpret equation (1) in amplitude and phase. In some cases (e.g., for VLF propagation during daytime from a ground-based transmitter), it is unnecessary to consider more than three modes; however more modes are needed for night-time propagation at the higher VLF frequencies [Snyder and Pappert, 1969; Bickel *et al.*, 1970; Pappert and Bickel, 1970].

The field strength due to each mode n depends on Λ_n and S_n. These factors depend on wavelength, ionosphere height, the ground electrical properties, and the spherical reflection coefficient of the ionosphere. The ionosphere reflection coefficients depend on the vertical distribution of electron density and collision frequency, the direction and magnitude of the Earth's magnetic field, the frequency, and angle of incidence. The electron density distribution is a function of latitude, season, solar cycle, time of day and whether or not ionospheric disturbances are present.

The influences of these various parameters can be broadly summarized in the following way [Al'pert *et al.*, 1967; Budden, 1961; Volland, 1966; Wait, 1964]:

- *Ground conductivity:* In general the effect of reducing the ground conductivity is to increase the attenuation rate of all modes. However, some calculations [Wait and Spies, 1965] show that when the conductivity is very low (e.g. polar ice-caps) the attenuation rate may approach a maximum and then decrease as the conductivity is lowered further. For moderate conductivities the magnitude of the excitation factor for the first order mode usually increases somewhat as the conductivity is reduced. Furthermore, as the conductivity is reduced, the phase velocity of each mode is also reduced.

- *Direction of propagation with respect to the Earth's magnetic field:* VLF model parameters show little variation with latitude or direction of propagation in the daytime. At night, there is little latitudinal variation for propagation to the magnetic east. For propagation to the magnetic west, all VLF propagation parameters show a strong latitudinal variation as the magnetic equator is approached. In particular, attenuation is greater for propagation to the west than to the east. The exact magnitude and form of the azimuthal variation in VLF propagation parameters at the magnetic equator has yet to be determined.

  Experimentally, observations of trans-equatorial anomalies over westerly trans-equatorial paths have been reported [Crombie, 1966; Lynn, 1967, 1969 and 1975; Kaiser, 1969; Chilton *et al.*, 1969; Meara, 1973; Reder, 1979] which suggest that the major variation occurs within some 15° of the magnetic equator. At Omega navigational frequencies, the diurnal phase shift on the east-to-west trans-equatorial path is 35% less than the average value at mid-latitudes [Lynn, 1975; Kikuchi, 1983]. Anomalous interference caused by a long-path signal takes place around the geomagnetic equator, indicating a large east-west asymmetry in the attenuation of propagation [Kikuchi and Ohtani, 1984]. Theoretical calculations have been presented [Gallenberger and Swanson, 1971] that show a major variation in model parameters for westward directions of propagation as the magnetic equator is approached. The frequency dependence of these effects has yet to be determined.

- *Use of conductivity parameter:* It has been shown [Wait and Spies, 1965] that useful calculations of wave-guide mode propagation can be performed by assuming the height variation of a conductivity parameter $\omega_r(z)$ to be given by:

$$\omega_r(z) = \omega_r(h) \exp [\beta (z - h)] \tag{3}$$

where $\omega_r = \omega_0^2/\nu$ for $\nu \gg \omega$; ω, ν and ω_0 are the wave angular frequency, the collision frequency, and plasma angular frequency respectively; z is the height, h is a reference height at which $\omega_r \simeq 2.5 \times 10^5\ s^{-1}$. The term β gives the vertical gradient of ω_r. Under daytime conditions, h is about 70 km and $\beta \approx 0.3$, while at night h is around 90 km and $\beta \approx 0.5$. These two parameters, h and β, provide a convenient, but approximate, means of describing the ionosphere for use in VLF calculations.

An extensive summary of specific values of the β and h parameters needed to simulate daytime and night-time VLF and LF propagated fields is given by Morfitt [1977] and by Davis and Berry [1977].

2.2 *Calculating field strength in a non-homogeneous guide*

The above calculations refer to conditions where the path properties are independent of distance. When the electron density distribution with height along the path is constant but the ground conductivity or magnetic field angle changes, it is approximately correct to use average values of the attenuation rate and phase velocity in performing the computation. For example, if the attenuation rates and phase velocities over a portion of the path of length d_m are α_{nm} and $c/\mathrm{Re}S_{nm}$ then

$$\alpha_d = \sum_m \alpha_{nm} d_m \tag{4}$$

$$\mathrm{Re}S_n d = \sum_m \mathrm{Re}\, S_{nm} d_m \tag{5}$$

When the reference heights of the ionosphere at the transmitter and receiver are different (near dawn or dusk), this procedure is not very accurate. It is then necessary, in addition, to replace Λ_n and h in equation (1) by $\sqrt{\Lambda_{nT}\,\Lambda_{nR}}$ and $\sqrt{h_T\,h_R}$ respectively, where the subscripts T and R refer to the transmitter and receiver locations [Wait, 1964; Watt, 1967].

The amplitude and phase of a single mode change smoothly in a non-oscillatory manner with distance. When two or more modes with different phase velocities are present, the field strength changes in an oscillatory manner as the various modes go in and out of phase. If only one mode is present $\Phi = \Phi_n - kd\,\mathrm{Re}S_n$. When more than one mode is present, it is suggested that calculations start with small distances and calculate new values of Φ with increasing distance.

An approximate procedure is available for calculating the diurnal field strength changes when signals are transmitted in an east-to-west or west-to-east direction and portions of the path are in daylight and darkness. This gives signal amplitudes and phases which are proportional to the combined day and night excitation factors $\Lambda_{D,N}$, attenuation rates, $\alpha_{D,N}$, and phase velocities, $V_{D,N}\,(c/\mathrm{Re}S_{D,N})$ as follows:

$$E_n \approx \sqrt{\frac{|\Lambda_D| \cdot |\Lambda_N|}{h_D \cdot h_N}}\; e^{-(\alpha_D d_D + \alpha_N d_N)}\, e^{i\left[\frac{\Phi_N + \Phi_D}{2} - k(S_N d_N + S_D d_D)\right]} \qquad (6)$$

Such an approach appears to account for the gross diurnal changes which are observed on long paths (approximately 10 000 km) at frequencies below about 18 kHz. The total phase delay is the sum of the phase delays along the sunlit and dark portions of the path. As the terminator (i.e. the sunrise or sunset line) moves along the path, the phase in this simple single mode model changes in proportion to the length of path in darkness giving rise to the well known trapezoidal diurnal variation [Crombie *et al.*, 1958].

At higher frequencies or on shorter paths, however, this approach is no longer adequate since it is found that the diurnal changes of phase may almost disappear, or even be reversed (i.e. phase delays are greater during the day than at night) or that the changes at sunrise and sunset may be in the same direction [Burgess, 1970]. However, when two or more modes are included in equation (1) and the calculations of phase delay are made for appropriate daytime and night-time parameters the observed patterns are obtained.

Another phenomenon [Crombie, 1964; Lynn, 1967; Walker, 1965] observed at sunrise or sunset is that instead of the phase changing smoothly, it changes in a series of steps which are accompanied by deep nulls in the field strength. This feature is observed at all frequencies in the VLF band and is not masked by the above-mentioned irregular behaviour at the lower frequencies and on long paths. The phase steps are a result of conversion of energy from one mode into another at the sunrise or sunset terminator. For example consider the case of propagation west to east at sunrise. The transmitter excites several modes of which at least the second and first are of significant amplitude at the terminator. However, because they travel with different phase velocities, they go in and out of phase along the path. The variation of mode conversion parameters with frequency has been experimentally determined by Lynn [1973].

Values of the mode parameters are best derived by fitting equation (1) to measurements of field strength versus distance taken during day and night conditions over a wide variety of paths [Wait, 1962; Watt, 1967; Bickel, 1967; Rhoads and Garner, 1967; Bickel *et al.*, 1970].

Considerable progress has been made in developing models which more correctly partition the radio energy into propagating modes through regions of rapid changes in the medium [Wait, 1968a, 1968b, 1970; Wait and Spies, 1968]. These mode conversion procedures are required for calculating the diurnal field strength changes when signals are transmitted across the daytime – night-time terminator region. Mode conversion procedures are also important when the medium changes along the propagation path (e.g., anomalous solar effects on the ionosphere or large changes in the ground conductivity).

A mode-conversion computer program has been developed which allows fully for the vertical inhomogeneity of the ionosphere as well as its anisotropy [Pappert and Snyder, 1972]. As an illustration of the potential use of the program at VLF, the sunrise amplitude of Walker [1965] was numerically modelled with allowance for four modes. Exponential profiles of varying reference height and scale height were used to simulate the terminator. Of the modelled studies, best agreement was obtained with a terminator thickness of 1000 km. Despite the multimode nature of the models, Crombie's [1964] model (where the first two night-time modes are converted into the first daytime mode) was found to be valid for the path studied because of weak conversion from the third and fourth night-time modes to the first daytime mode. Crucial to the solution of waveguide problems that involve inhomogeneity in the direction of propagation is the ability to represent the field components as an expansion in a complete set of waveguide modes [Pappert and Smith, 1972]. Evaluation of the coefficients in such an expansion generally makes use of the orthogonality of modes for the given waveguide and those of an appropriate "adjoint" waveguide.

This mode conversion program also gives good agreement to experimental sunrise results obtained with a multiple frequency VLF ionospheric sounder over a propagation path from Hawaii to southern California [Pappert and Morfitt, 1975]. Contrary to the Crombie hypothesis [Crombie, 1964], two modes were found to be influential when the receiving site was located in the daytime part of the path.

The width and the location of the change in effective waveguide height in going from day to night at sunrise and sunset are discussed by Pappert and Snyder [1972] and Lynn [1973]. Detailed calculations of sunrise phase and amplitude parameters arising from mode conversion have been compared with observation [Rugg, 1967; Mahmoud and Beal, 1971; Rinnert, 1973; Suzuki *et al.*, 1973].

The modal interference spacing (the distance over which the phase difference between two propagation modes changes by one phase cycle (2π)) is a theoretically calculable parameter which can be measured with great accuracy. Experimental determinations for the two most significant modes have been given as a function of frequency for day or night conditions [Steele and Crombie, 1967; Rawles and Burgess, 1967] and for a range of latitudes [Lynn, 1977]. Modal interference spacings determine the location of signal minima observed in aircraft flights, the timing of signal minima and of the steps in phase during sunrise and sunset, and the regular variations in diurnal phase magnitude and day-to-night signal levels with distance [Kaiser, 1969] and frequency [Araki, 1973; Lynn, 1978].

VLF radio waves propagating across Greenland are strongly affected by the very poor conductivity of the ice cap; see for example, the signal strength data of Burgess, obtained aboard aircraft flying across Greenland [Morfitt, 1977]. Experimental data show that when the ionospheric reflection height decreases, both attenuation and phase velocity increase more than normal for a seawater path [Crombie, 1967; Westerlund *et al.*, 1969]. It is found theoretically [Westerlund and Reder, 1973] that the ice affects all the important (quasi-TM) modes. Compared to seawater propagation, the first order mode has a higher phase velocity over ice, while second and third order modes have lower velocities. All three modes have higher attenuation. Mode conversion effects at the abrupt change in ground conductivity at the Greenland coast are important.

3. Calculating field strength by waveguide modes: full wave solution

In the propagation of ELF, VLF and LF terrestrial radio waves to great distances, the waves are confined within the space between the earth and the ionosphere. This space acts as a waveguide, and the "waveguide concept" is applicable for characterizing the propagated fields as a function of distance.

The waveguide mode method obtains the full wave solution for a waveguide that has the following characteristics:

- arbitrary electron and ion density distributions and collision frequency (with height) and
- a lower boundary which is a smooth homogeneous earth characterized by an adjustable surface conductivity and dielectric constant. This method also allows for earth curvature, ionospheric inhomogeneity, and anisotropy (resulting from the earth's magnetic field).

The energy within the waveguide is considered to be partitioned among a series of modes. Each mode represents a resonant condition, i.e., for a discrete set of angles of incidence of the waves on the ionosphere, resonance occurs and energy will propagate away from the source. The complex angles (θ) for which this occurs are called the eigenangles (or "modes"). They may be obtained using the "full-wave" procedures described in §§ 3.1 and 3.2 by solving the determinantal equation (i.e., the modal equation):

$$F(\theta) = \left| R_d(\theta)\, \overline{R}_d(\theta) - 1 \right| = 0 \tag{7}$$

where

$$R_d(\theta) = \begin{bmatrix} {}_{\parallel}R_{\parallel d}(\theta) & {}_{\perp}R_{\parallel d}(\theta) \\ {}_{\parallel}R_{\perp d}(\theta) & {}_{\perp}R_{\perp d}(\theta) \end{bmatrix} \tag{8}$$

is the complex ionospheric reflection coefficient matrix looking up into the ionosphere from height "d" and

$$\overline{R}_d(\theta) = \begin{bmatrix} {}_{\parallel}\overline{R}_{\parallel d}(\theta) & 0 \\ 0 & {}_{\perp}\overline{R}_{\perp d}(\theta) \end{bmatrix} \tag{9}$$

is the complex reflection matrix looking down from height "d" towards the ground.

The notation $_{\parallel}$ for the R's and $\overline{R}$'s denotes vertical polarization while the notation $_{\perp}$, denotes horizontal polarization. The first subscript on the R's referes to the polarization of the incident wave while the second applies to the polarization of the reflected wave.

The individual terms of equations (8) and (9) are:

$_{\parallel}R_{\parallel}$: the ratio of the reflected field in the plane of incidence to the incident field in the same plane.

$_{\perp}R_{\perp}$: the ratio of the reflected field perpendicular to the plane of incidence to the incident field perpendicular to the plane of incidence.

$_{\parallel}R_{\perp}$: the ratio of the reflected field perpendicular to the plane of incidence to the incident field in the plane of incidence.

$_{\perp}R_{\parallel}$: the ratio of the reflected field in the plane of incidence to the incident field perpendicular to the plane of incidence.

The ionospheric reflection matrix, R_d (equation (8)) at height, d, is obtained by numerical integration of differential equations given by Budden [1955]. The differential equations are integrated by a Runge-Kutta technique, starting at some height above which negligible reflection is assumed to take place. The initial condition for the integration, i.e., the starting value of R, is taken as the value of R for a sharply-bounded ionosphere at the top of the given electron density and collision frequency profiles. The method for obtaining this starting solution is described by Sheddy [1968]. The term R_d is calculated as described by Pappert *et al.* [1967] in terms of solutions to Stokes equation and their derivatives.

The modal equation, equation (7), is solved for as many modes (eigenangles, θ_n) as desired. From the set of θ's so obtained the propagation parameters: attenuation rate, phase velocity and the magnitude and phase of the excitation factor, can be computed [Pappert *et al.*, 1967]. These parameters are then used in a modal summation to compute the total field, amplitude and phase, at some distant point.

In many instances, the earth-ionosphere waveguide can be considered to have constant propagation properties along the transmission path. The mode sum calculations made for these cases are referred to as horizontally homogeneous. However, for propagation to great distances it is unrealistic to assume the waveguide parameters will remain constant along the whole length of the path. For example, the direction and strength of the Earth's magnetic field will vary and discontinuities can occur in the lower wall of the waveguide due to the presence of ground conductivity changes associated with various land-sea boundaries and the polar ice caps. The ionospheric conductivity also varies according to the time of day, season and the presence of the sunrise or sunset line along the propagation path.

These types of discontinuities are those which cause discrete changes in the waveguide. In these cases mode conversion effects at the discontinuity must be taken into consideration. Mode conversion implies that a single mode propagating in one region of the waveguide will produce two or more modes in the other section of the guide which then propagate to the receiver.

3.1 *The ionospheric reflection matrix, R(θ)*

A crucial step in the determination of the mode constants discussed in the previous section is the evaluation of the reflection matrix R for a vertically inhomogeneous anisotropic ionosphere. This is achieved by a numerical integration of differential equations given by Budden [1955].

The coordinate system chosen is such that the direction of z is taken positive into the ionosphere. Positive x is the direction of propagation and y is normal to the plane of propagation.

The geometry is shown in Fig. 1 where a plane wave is shown incident upon the ionosphere from below with wave vector $\vec{k}$ in the x-z plane (plane of incidence) at an angle of incidence θ_1 to the vertical (z-axis). Other variables identified in the figure are Ω, the angle of the geomagnetic field measured from the vertical ($90° < \Omega \leqslant 180°$ for the Northern Hemisphere), and ψ, the azimuth of propagation (east of magnetic north). The vector $\vec{B}$ is the earth's magnetic flux density.

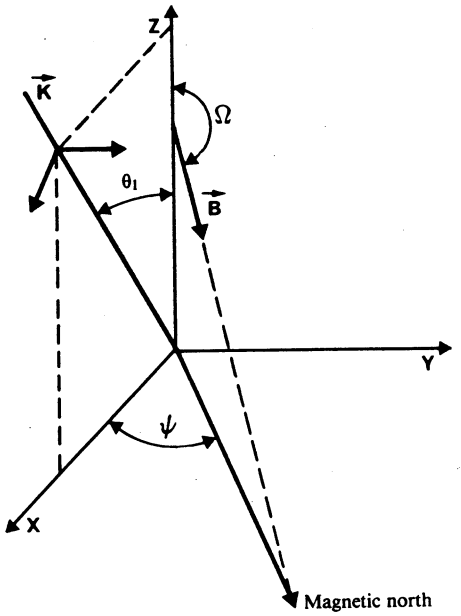

FIGURE 1 – *Wave propagation geometry*

The differential equations are integrated by a Runge-Kutta technique starting at some height above which neglible reflection is assumed to take place. The starting value of R is the value of R for a sharply bounded homogeneous ionosphere characterized by parameters at the top of the given electron, ion and collision frequency profiles. The solution used for the initial R is that described by Sheddy [1968]. Error control in the Runge-Kutta integration is by means of comparison for each step of the increments in the elements of R computed with a fourth-order Runge-Kutta method and those computed with a second-order integration step. The integration is carried out from some starting height down to the height d, where d is identified in equation (7). It is necessary only that d be chosen sufficiently low in the ionosphere that ionospheric effects are small relative to earth-curvature effects. Below level d the only effect is that of earth curvature which is included by introducing a modified permittivity which varies linearly in height.

3.2 *The ground reflection matrix,* $\overline{R}_d(\theta)$

The ground reflection coefficient matrix $\overline{R}_d$, as given in equation (9), is determined in terms of independent solutions, h_1 and h_2 to Stokes' equation

$$\frac{d^2 h_{1,2}}{dz^2} + z h_{1,2} = 0 \tag{10}$$

where the functions h_1 and h_2 are modified Hankel functions of order 1/3 (which are linearly related to Airy functions) as defined by the Computation Laboratory, Cambridge [1945]. The explicit expressions for $_{\|}\overline{R}_{\|}$ and $_{\perp}\overline{R}_{\perp}$ are given by [Pappert *et al.*, 1967].

3.3 *The mode finding method* ("MODESRCH")

Waveguide theory treats the field as being composed of one or more discrete families (modes) of plane waves confined to the earth-ionosphere waveguide. The principle objective is to find solutions to equation (7) for the eigenangles θ_n. To achieve this a method known as "MODESRCH" [Morfitt and Shellman, 1976] is employed.

The "MODESRCH" method, developed primarily for VLF and lower LF (10 kHz to about 60 kHz) propagation in the earth-ionosphere waveguide finds all modes in any physically important rectangular region of the complex eigenangle (θ_n) space. The method also finds the single mode needed for ELF propagation. The procedure is based on complex variable theory. The modal equation, equation (7), is solved for all the important eigenangles, θ_n, for the given set of earth-ionosphere parameters and propagation frequency. The search for the eigenangles is based on the fact that the lines of constant phase for any complex function, $F(\theta)$, may be discontinuous only at points where $F\theta = 0$ or $F(\theta) \rightarrow \infty$. To simplify the problem of finding the θ_n values, the function $F(\theta)$ is modified so that it contains no poles and only $F(\theta) = 0$ is considered. A solution of $F(\theta) = 0$ is denoted by θ_0, i.e., θ_0 is a zero of $F(\theta) = 0$.

Let:

$$F(\theta) = F_R(\theta_r, \theta_i) + j\, F_I(\theta_r, \theta_i) = \text{Re}\,(F) + j\,\text{Im}\,(F) \tag{11}$$

where

$$\theta = \theta_r + j\theta_i \tag{12}$$

Also

$$F(\theta) = [F_R(\theta_r, \theta_i)^2 + F_I(\theta_r, \theta_i)^2]^{1/2}\, e^{j\theta} \tag{13}$$

where

$$\varphi = \tan^{-1}\left[\frac{F_I(\theta_r,\theta_i)}{F_R(\theta_r,\theta_i)}\right] \tag{14}$$

and

$F_R(\theta)$: the real part of the complex function $F(\theta)$,

$F_I(\theta)$: the imaginary part of the complex function $F(\theta)$,

θ_r : the real part of the complex angle (θ),

θ_i : the imaginary part of the complex angle (θ).

From equation (14) if

$\varphi = 0°$ (or 180°), this implies that

$F_I(\theta_r,\theta_i) = 0$

Also if

$\varphi = 90°$ (or 270°), this implies that

$F_R(\theta_r,\theta_i) = 0$

This leads to the phase diagram of Fig. 2. A set of lines of constant phase referred to as phase contours ranging from 0 to 2π radians emanates radially (solid lines) from a simple zero. The dashed lines depict possible phase contour behaviour, in the region beyond the neighbourhood of θ_0, in order to emphasize that in this region the phase contours are generally not radial. In view of the phase behaviour near a zero of $F(\theta)$ it is conceptually useful to define a zero of $F(\theta)$ as a set of phase contours.

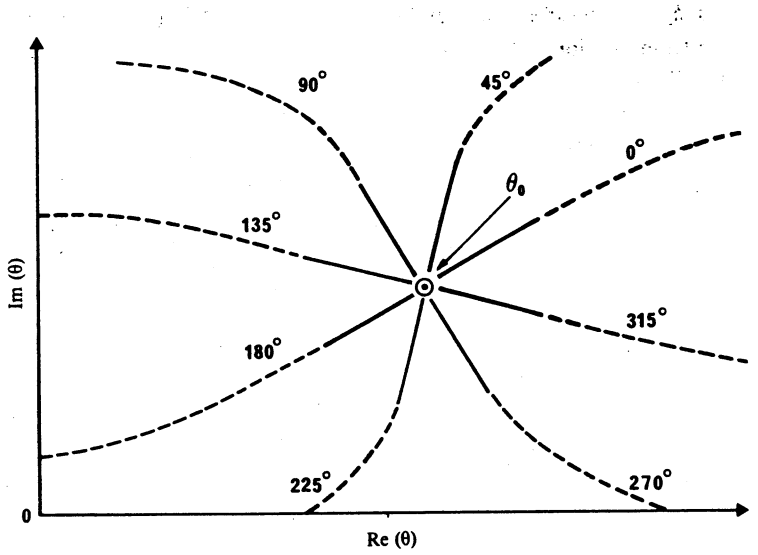

FIGURE 2 – *Phase contour behaviour near a zero of F (θ)*

——— phase contour in the neighbourhood of θ_0

– – – – phase contour beyond the neighbourhood of θ_0

Some fundamentals of the procedure to find zeros of the function, $F(\theta)$, are illustrated in Fig. 3. A search rectangle is placed about some region of the complex plane. The search rectangle is divided into a grid of mesh squares whose corners will be called mesh points. The mesh square size is optional and is usually selected according to the expected zero spacing. If $F(\theta)$ has no poles, this implies that the line of any particular constant phase value $\varphi = \varphi_c$, radiating from a zero of $F(\theta)$, must cross a closed contour containing that zero at least once. Furthermore, no other zero of $F(\theta)$ may be on this phase line. Also, the lines of constant phase around $F(\theta) = 0$ progress only in a counterclockwise direction. A line of constant phase (e.g., $\varphi = \varphi_c$) which crosses the contour may be followed inward until it leads to a zero of $F(\theta)$ or until the line again reaches the contour. Beginning at the upper left corner of the search rectangle, a boundary search for 0° and 180° phase contours is conducted in a counterclockwise direction. Any phase contour would do; however, the 0° and 180° phase contours are selected because mathematically they are easily located, occurring when Im $(F) = 0$. The search is conducted by evaluating $F(\theta)$ at the mesh points along the search rectangle boundary. When Im (F) changes sign, it indicates that a 0° or 180° phase contour has just been passed (points A, D, and G). Once either of these phase contours is located, the boundary search is temporarily halted while the 0° or 180° phase contour is traced into the interior of the search rectangle by inspection of Im $F(\theta)$ at the corners of the mesh squares (counterclockwise inspection beginning at the top left corner of each mesh square). The phase contour is followed either until a zero of $F(\theta)$ is discovered (points B and E) or until the search rectangle boundary is encountered (as would be the case for the phase contour between G and H), one of which will always occur provided no poles exist in the interior of the search rectangle. When a zero is located its location is saved. Then the phase contour is traced out the opposite side of the zero, having undergone a 180° phase change (see Fig. 2), until the search rectangle boundary is again encountered (points C and F). When the phase contour exists the search boundary, such as at points C, F, or H, the mesh square which contains this occurrence is flagged so as to avoid following the particular phase contour again at a later time during the boundary search. Also at such a point (point C, F, or H) the phase contour trace is stopped and the boundary search is resumed at the point where the last 0° or 180° phase line was encountered (e.g., points A, D, or G). Once the entire search rectangle boundary has been inspected, all the zeros of the function $F(\theta)$, located within the search rectangle will have been found.

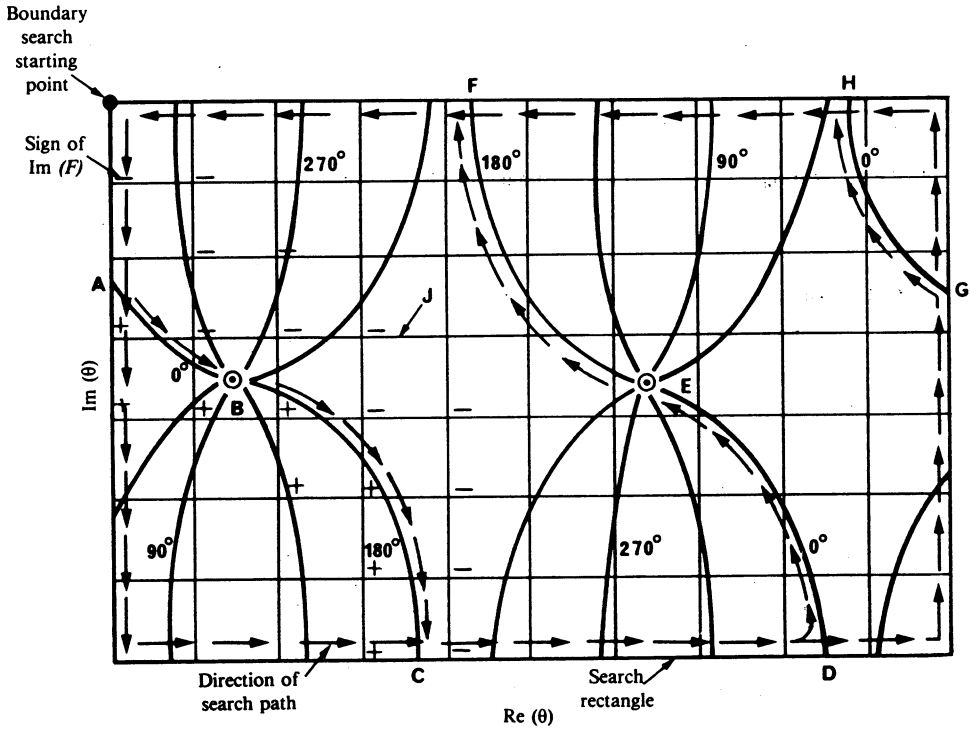

FIGURE 3 – *Mode finding method for the function F(θ)*

——— phase contours for $F(\theta)$

⊙ zeros of $F(\theta)$

J mesh square

The location of a zero is evident by the intersection of phase contours (see Fig. 2). Therefore, the intersection of the 0° or 180° phase contour with any other phase contour locates a zero of $F(\theta)$. The other phase contour chosen for this purpose is the 90° or 270° phase contour, again chosen for simplicity, as these contours are easily recognized, occurring when Re $(F) = 0$. While a 0° or 180° phase contour is being traced, Re (F) is also examined at the corners of each mesh square to locate a Re (F) sign change which indicates that a 90° or 270° phase contour has entered the mesh square. Such an occurrence indicates that a zero is probably within that mesh square or perhaps within an adjacent mesh square. Once a mesh square is known to contain a zero, a more precise location of the zero is obtained by an interpolation scheme which employs both the magnitude and phase of the function $F(\theta)$. Following this a Newton-Raphson iteration pinpoints the location of the zero.

The Newton-Raphson procedure is to use each of the eigenangle solutions, θ_n, as obtained from the "MODESRCH" grid as a starting solution θ_0 to equation (7) where $F(\theta) = 0$. The function is then re-evaluated for $\theta_0 + \delta\theta$ and the correction to θ_0 found from the equation

$$\Delta\theta = - \frac{F(\theta_0)\,\delta\theta}{F(\theta_0 + \delta\theta) - F(\theta_0)} \tag{15}$$

The correction determined by equation (15) is then evaluated and the process repeated until the quantities $|\Delta\theta_r|$ and $|\Delta\theta_i|$ are reduced to within a pre-assigned tolerance. The subscripts r and i denote the real and imaginary parts, respectively.

A computer program is available to compute these eigenangles for an arbitrary ionosphere and a homogeneous earth [Morfitt and Shellman, 1976].

4. Calculation of field strength

4.1 *Required parameters*

With the eigenangles, θ_n, known, the following quantities of physical interest are readily calculated.

$$V = \frac{c}{K(\sin\theta_n)_r} \quad = \text{phase velocity at the ground} \tag{16}$$

$$\Gamma = -8.6859kK(\sin\theta_n)_i \quad = \text{attenuation constant at the ground (in dB/megameter)} \tag{17}$$

where

$$c = 2.997928 \times 10^5 \text{ km/s} \quad = \text{vacuum speed of light}$$

$$K = \left(1 + \frac{\alpha h}{2}\right) \tag{18}$$

$$\alpha = 2/a = 3.14 \times 10^{-4}/\text{km} \tag{19}$$

Using the geometry of Fig. 1 the direction of stratification is the z direction and the direction of propagation is in the x-z plane. The direction of z is taken positive into the ionosphere. Positive x is the direction of propagation and y is normal to the plane of propagation. Thus, the fields exhibit no y dependence and a dependence on x of the form $\exp(-ik\sin\theta_x)$ where k is the magnitude of the free-space propagation vector and θ is the angle between the direction of the propagation vector and the z direction at a point in the stratified medium where the modified index of refraction is unity. All field quantities are assumed to have an $\exp(i\omega t)$ dependence where ω is the angular frequency.

The modal excitation factor and the modal height gain functions are two parameters needed in computing electric field strengths. The excitation factor formulae, are summarized in Table I. The column headings only apply to excitation of the electric field components E_z, E_y and E_x and the row headings apply to excitation by a vertical dipole (λ_V), horizontal dipole end on (λ_E) and a horizontal dipole broadside (λ_B).

R and $\overline{R}$ represent, respectively, elements of the reflection matrix looking into the ionosphere and towards the ground from the same level d within the guide. B_1 and B_2 are given by

$$B_1 = \frac{S^{5/2}}{\left.\frac{\alpha F}{\alpha\theta}\right|_{\theta-\theta_n}} \qquad B_2 = -\frac{B_1}{S} \tag{20}$$

where S is the sine of the eigenangle and the denominator is the derivative of the modal equation at the eigenangle, θn.

TABLE I — *Excitation factors*

Field component	E_z	E_y	E_x
Exciter			
λ_V	$B_1 \dfrac{(1+{}_{\parallel}\bar{R}_{\parallel})^2(1-{}_{\perp}\bar{R}_{\perp}\,{}_{\perp}R_{\perp})}{{}_{\parallel}\bar{R}_{\parallel}\,D_{11}}$	$\dfrac{-B_1}{S}\dfrac{{}_{\parallel}R_{\perp}(1+{}_{\parallel}\bar{R}_{\parallel})(1+{}_{\perp}\bar{R}_{\perp})}{D_{12}}$	$\dfrac{B_1}{S}\dfrac{(1+{}_{\parallel}\bar{R}_{\parallel})^2(1-{}_{\perp}\bar{R}_{\perp}\,{}_{\perp}R_{\perp})}{{}_{\parallel}\bar{R}_{\parallel}\,D_{11}}$
λ_E	$B_2 \dfrac{(1+{}_{\parallel}\bar{R}_{\parallel})^2(1-{}_{\perp}\bar{R}_{\perp}\,{}_{\perp}R_{\perp})}{{}_{\parallel}\bar{R}_{\parallel}\,D_{11}}$	$\dfrac{-B_2}{S}\dfrac{{}_{\parallel}R_{\perp}(1+{}_{\parallel}\bar{R}_{\parallel})(1+{}_{\perp}\bar{R}_{\perp})}{D_{12}}$	$\dfrac{B_2}{S}\dfrac{(1+{}_{\parallel}\bar{R}_{\parallel})^2(1-{}_{\perp}\bar{R}_{\perp}\,{}_{\perp}R_{\perp})}{{}_{\parallel}\bar{R}_{\parallel}\,D_{11}}$
λ_B	$B_2 \dfrac{{}_{\perp}R_{\parallel}(1+{}_{\perp}\bar{R}_{\perp})(1+{}_{\parallel}\bar{R}_{\parallel})}{D_{12}}$	$\dfrac{-B_2}{S}\dfrac{(1+{}_{\perp}\bar{R}_{\perp})^2(1-{}_{\parallel}\bar{R}_{\parallel}\,{}_{\parallel}R_{\parallel})}{{}_{\perp}\bar{R}_{\perp}\,D_{22}}$	$\dfrac{B_2}{S}\dfrac{{}_{\perp}R_{\parallel}(1+{}_{\perp}\bar{R}_{\perp})(1+{}_{\parallel}\bar{R}_{\parallel})}{D_{12}}$

The excitation factors must be supplemented with definitions of the height gains.

The field-strength calculations can be made for electric dipole exciters of arbitrary orientation located at any height within the guide. Thus, air-to-air, ground-to-air or air-to-ground VLF/LF propagation problems involving a horizontally inhomogeneous waveguide channel may be treated. Figure 4 shows the dipole orientation relative to the propagation geometry in which the z axis is always normal to the curved earth surface. The angles γ and φ measure the orientation of the transmitter relative to the x, y, z coordinate system.

From Fig. 4, $\gamma = 0°$ represents the excitation from a vertical dipole while $\gamma = 90°$ gives the excitation from a horizontal dipole. Also φ is the angle between the direction of the horizontal dipole and the direction of propagation. Explicitly, $\varphi = 0$ represents end fire and $\varphi = 90°$ represents broadside launching.

4.2 *WKB and horizontally homogeneous mode sums*

In addition to the vertical inhomogeneity of the ionosphere the guide may exhibit horizontal inhomogeneity. In particular, variability in propagation constants along the great circle path of propagation can result from either horizontal variability of the ionosphere, from variability of the ground conductivity and/or permittivity, as well as from variations in the geomagnetic field strength or orientation. In instances for which the earth ionosphere waveguide cannot be considered as horizontally homogeneous along the propagation path, a WKB form of the mode sum is used. This model is accurate when changes in the modal parameters are sufficiently gradual along the path.

In terms of the excitation factors and height gains, the WKB mode sum equations may be written as a function of propagation distance.

If the propagation path may be considered as horizontally homogeneous along its entire length, the equation becomes much simpler:

$$(\lambda_V^T = \lambda_V^R), (\lambda_B^T = \lambda_B^R) \text{ and } (\lambda_E^T = \lambda_E^R). \qquad \text{Also, } (\bar{S}_n^T = \bar{S}_n^R)$$

which may be used to compute the fields for multimode propagation at VLF and LF frequencies. These equations may also be used for ELF frequencies, however, because of the small attenuation rates which prevail in the lower ELF band, significant interference between the long and short path signals can occur.

Computer programs are available to compute these field strengths. These are for VLF/LF [Pappert and Shockey, 1971] and for ELF [Pappert and Shockey, 1972a and 1972b].

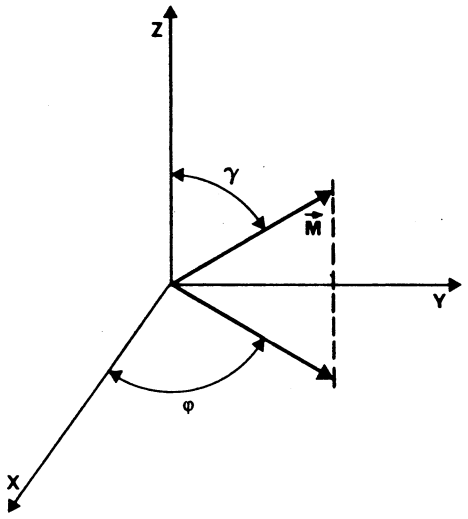

FIGURE 4 – *Dipole $\vec{M}$ orientation within the waveguide where γ is the inclination and φ the azimuthal orientation*

4.3 *Mode sums using mode conversion*

For those propagation conditions where the properties of the earth-ionosphere waveguide can not be considered as slowly varying, mode conversion techniques must be utilized. Examples, where mode conversion procedures are required for calculating field strengths, are for transmissions across the daytime-night-time terminator region or when the propagation path consists of large changes in ground conductivity, such as the transition from land to sea. The mode conversion model allows for an arbitrary number and order of modes on each side of the waveguide discontinuity. This model also allows for the calculation of the horizontal, as well as the vertical, component of the electric field at an arbitrary height in the waveguide.

The mode conversion program is based on the slab model shown in Fig. 5. Invariance in the y direction is assumed and reflection from the horizontal inhomogeneity is neglected. Subject to these assumptions and to the assumption of a unit amplitude wave in mode k incident in the transmitter region (slab NTR) the generalized mode conversion coefficient a_k^p for the p^{th} slab associated with conversion from the kth to the j^{th} mode expressed in terms of the coefficients for the previous $(p+1)^{th}$ slab may be written in the form:

$$\sum_{j=1}^{J} a_{ik}^{p} I_{n,j}^{p,p} = I_{n,k}^{p,p+1} \qquad p = NTR - 1$$

$$= \sum_{j=1}^{J} a_{jk}^{p+1} \left[-iks_j^{p+1} (x_p - x_{p+1}) \right] I_{n,k}^{p,p+1} \qquad 1 \leqslant p < NTR - 1 \qquad (21)$$

where $i = (-1)^{1/2}$, k is the free-space wave number, S_j is the sine of the jth eigenangle for the pth slab, and J is the total number of modes assumed to be important in the total field determinations.

Critical for the solution of the system of equations (21) is the evaluation of the integral:

$$I_{jk}^{m,p} = \int_{-\infty}^{\infty} A_j^{mt} \cdot G_k^p \, dz \qquad (22)$$

where the t denotes the adjoint factor and G^p a four-element column matrix of height gains for the y and z components of the electric and magnetic field strength of the kth mode in the pth slab.

The term A_j^m is a four-element column matrix of height gains for an appropriate adjoint waveguide [Pappert and Smith, 1972].

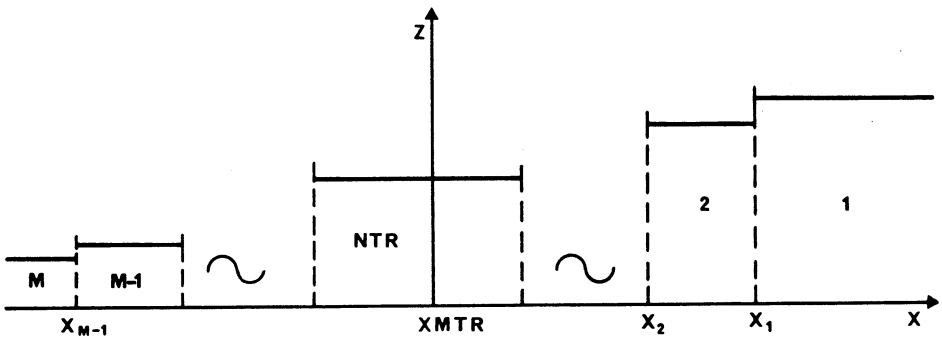

FIGURE 5 – *Mode conversion model*

Again, as in the case of the WKB mode sum procedure, the field-strength calculations can be made for electric dipole exciters of arbitrary orientation located at any height within the guide. Thus, air-to-air, ground-to-air or air-to-ground VLF/LF propagation problems in a horizontally inhomogeneous waveguide channel may be treated.

Two distinct options are available with the mode conversion procedure. One is for field calculations (amplitude and phase) as a function of range for a fixed location of the horizontal inhomogeneity. The second allows for field calculations at a distinct receiving point along a great circle path as a function of position of the horizontal inhomogeneity (this option is useful only if the ground conductivity and the geomagnetic parameters are invariant over the path). Amplitude is expressed in dB above a microvolt per metre for a one kilowatt radiator and phase in degrees relative to free space. A computer program is available for these mode conversion calculations [Pappert and Shockey, 1976].

4.4 *Ionospheric parameters*

The required ionospheric parameters needed to compute ELF/VLF/LF field strength values are the following profiles, which are functions of ionospheric height, Z. These are electron density profile, positive and negative ion density profiles, electron-neutral particle collision frequency profile and positive and negative ion-neutral particle collision frequency profiles.

A convenient parameter based on the above profiles is the ionospheric conductivity ω_r, which is a function of height, Z. This parameter is given by:

$$\omega_r(Z) = \frac{\omega_p^2(Z)}{\nu(Z)} = \frac{q^2}{\varepsilon_0}\left[\frac{N_e(Z)}{m_e \nu_e(Z)} + \frac{N_+(Z)}{m_+ \nu_+(Z)} + \frac{N_-(Z)}{m_- \nu_-(Z)}\right] \tag{23}$$

where

$\omega_p(Z)$: the plasma frequency,

q: the electron charge,

ε_0: the permittivity of free space,

ν_e: electron-neutral particle collision frequency (s^{-1}),

ν_+: positive ion-neutral particle collision frequency (s^{-1}),

ν_-: negative ion-neutral particle collision frequency (s^{-1}),

N_e: electron density (cm^{-3}),

N_+: positive ion density (cm^{-3}),

N_-: negative ion density (cm^{-3}),

m_e: mass of the electron,

m_+: mass of the positive ions,

m_-: mass of the negative ions.

For most cases of propagation at VLF or LF, only the electron density profile and electron-neutral particle collision frequency profile need to be considered. In this instance, following Wait and Spies [1965], the conductivity parameter $\omega_r(Z)$ may be considered of exponential form:

$$\omega_r(Z) = \omega_0 \exp[\beta (Z - H')] \tag{24}$$

where

β: a gradient parameter in inverse height units,

and

H': a reference height.

The ionospheric parameters needed as inputs to the multimode computer programs, then, are the electron density profile and the effective electron-neutral particle collision frequency profile. These terms may be assigned exponential relationships with height and are identified by the terms β, km^{-1} and H', km.

The value of the electron density $N(Z)$, in electrons/cubic centimetres is calculated as a function of height Z in kilometres by the equation:

$$N(Z) = \left\{1.43 \times 10^7 \times \exp(-0.15\,H')\right\}\left\{\exp[(\beta - 0.15)(Z - H')]\right\} \quad \text{el/cm}^3 \tag{25}$$

The collision frequency profile for the computations is:

$$\nu(Z) = \nu_0 \exp(-\alpha Z) \tag{26}$$

where

Z: the height in km,

ν_0: 1.82×10^{11} collisions/sec,

α: $0.15\ km^{-1}$.

This combination of electron density and collision frequency gives an ionospheric conductivity profile given by

$$\omega_r(Z) = 2.5 \times 10^5 \exp[\beta (Z - H')] \tag{27}$$

The usefulness of this simple ionospheric model is a result of its ease of application and its success in modelling experimentally measure data as demonstrated by Bickel *et al.*, [1970], Morfitt [1977], and Ferguson [1980]. The determination of the values of the β and H' parameters is achieved by comparing measured data with theoretical calculations, adjusting the parameters in the latter until acceptable agreement is obtained. The most straightforward method of comparison is obtained when the measured data are collected at a large number of points along a great circle propagation path which includes the transmitter. The easiest way to collect such data is aboard an aircraft. The data examined by Bickel *et al.*, Morfitt and Ferguson were collected in this way.

In general, the ionospheric models determined from the above procedure must be considered to represent an averaged ionosphere since the modelling assumes that the ionosphere was static during any aircraft flight period. The data fitting procedure attempts to find a calculated pattern of amplitude as a function of distance which agrees with the large scale pattern of the measured data. Thus, many small amplitude variations are averaged. It is possible that profiles of more complex forms than the exponential could be found to produce a better fit to measured data in some instances, but since the propagation paths considered are quite long, any profile determined to produce a best fit to the data is really an average profile for the total path.

Analysis of the available measured data suggests the following tables of ionospheric parameters for VLF/LF propagation predictions, Morfitt [1977] and Ferguson [1980].

The characteristic relationship, as a function for some exponential profiles is illustrated in Fig. 6 for daytime conditions and in Fig. 7 for night-time conditions.

For propagation at ELF, suggested electron and ion density profiles, [Pappert and Moler, 1974], are shown in Fig. 8.

Tables of suggested electron and ion collision profiles for ELF are given in Tables IV and V.

TABLE II — *Recommended profiles for daytime propagation at VLF/LF*

	Summer	Winter
High latitude	$\beta = 0.3$, $H' = 72$	$\beta = 0.3$, $H' = 72$
Middle latitude	$\beta = 0.5$, $H' = 70$	$\beta = 0.3$, $H' = 72$

TABLE III — *Recommended profiles for night-time propagation at VLF-LF*

Winter profiles					
	Magnetic dip range (degrees)	H' (km)		β (km^{-1})	
		F = 10-30 kHz	F = 30-60 kHz	F = 10-30 kHz	F = 30-60 kHz
High latitudes	90 to 75	76	76	$0.035F - 0.025$	1.2
Transition region	75 to 70	80	80	$0.035F - 0.025$	1.2
Middle latitudes	< 70	87	88	$0.0077F + 0.31$	$0.0077F + 0.31$
Summer profiles					
All latitudes		$H' = 87$		β (km^{-1}) = $0.0077F + 0.31$	

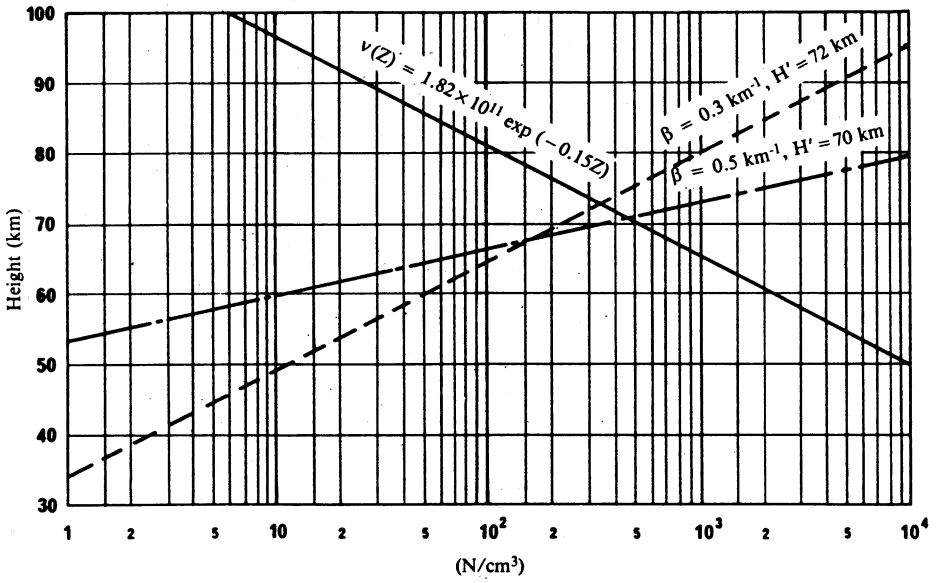

FIGURE 6 – *Daytime electron density profiles and collision frequency profile*

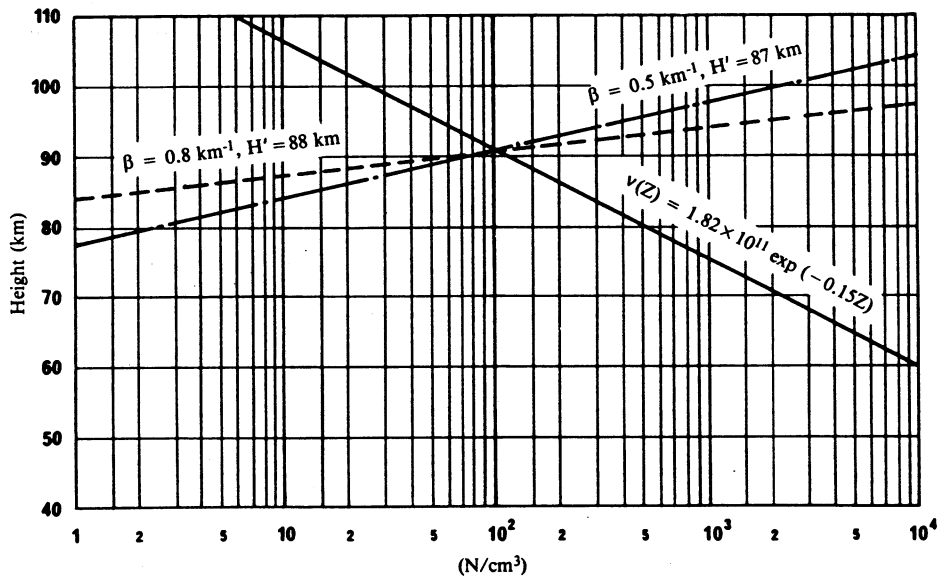

FIGURE 7 – *Night-time electron density profiles and collision frequency profile*

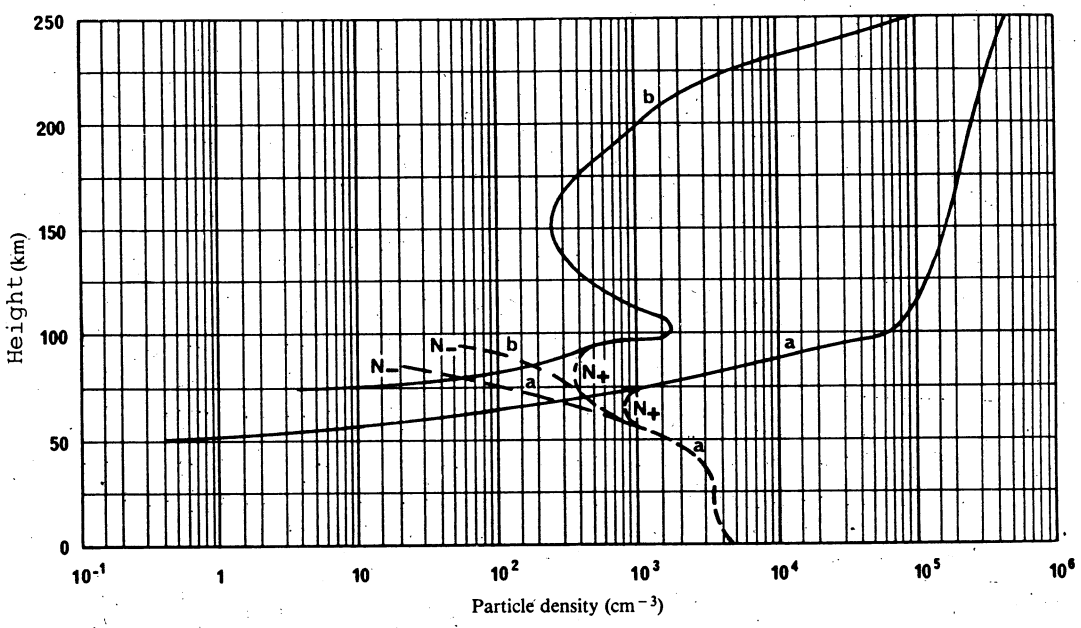

FIGURE 8 – *Ambient day and night constituent profiles*

——— electrons
– – – – ions
a day
b night

TABLE IV — *Daytime ionospheric electron and ion collision frequency in seconds^{-1} versus altitude*

Altitude (km)	Electrons	Positive ions	Negative ions
260	$6.6 \cdot 10^2$	1.02	1.02
230	$5.3 \cdot 10^2$	2.00	2.00
210	$4.8 \cdot 10^2$	3.10	3.10
200	$5.0 \cdot 10^2$	4.00	4.00
180	$6.0 \cdot 10^2$	$1.30 \cdot 10^1$	$1.30 \cdot 10^1$
170	$8.0 \cdot 10^2$	$2.40 \cdot 10^1$	$2.40 \cdot 10^1$
150	$1.6 \cdot 10^3$	$9.00 \cdot 10^1$	$9.00 \cdot 10^1$
120	$1.0 \cdot 10^4$	$6.00 \cdot 10^2$	$6.00 \cdot 10^2$
100	$3.9 \cdot 10^4$	$1.60 \cdot 10^4$	$1.60 \cdot 10^4$
0	$4.3 \cdot 10^{11}$	$2.14 \cdot 10^{10}$	$2.14 \cdot 10^{10}$

TABLE V — *Night-time ionospheric electrons and ion collision frequency in seconds^{-1} versus altitude*

Altitude (km)	Electrons	Positive ions	Negative ions
250	$1.05 \cdot 10^2$	$4.50 \cdot 10^1$	$4.50 \cdot 10^1$
225	$3.50 \cdot 10^1$	$9.00 \cdot 10^1$	$9.00 \cdot 10^1$
220	$3.00 \cdot 10^1$	1.00	1.00
210	$3.30 \cdot 10^1$	1.30	1.30
200	$4.50 \cdot 10^1$	2.00	2.00
150	$1.60 \cdot 10^3$	$4.50 \cdot 10^1$	$4.50 \cdot 10^1$
120	$1.00 \cdot 10^4$	$3.00 \cdot 10^2$	$3.00 \cdot 10^2$
100	$3.90 \cdot 10^4$	$8.00 \cdot 10^3$	$8.00 \cdot 10^3$
0	$4.30 \cdot 10^{11}$	$1.07 \cdot 10^{10}$	$1.07 \cdot 10^{10}$

4.5 *Geomagnetic and geophysical parameters*

Other parameters needed for the calculation of ELF/VLF/LF signal levels are those which describe the orientation and strength of the Earth's magnetic field along the propagation path, as well as those parameters which give the value of the Earth's complex dielectric constant as a function of propagation frequency.

The parameters which describe the Earth's magnetic field are the magnitude of the geomagnetic field, the magnetic azimuth (in degrees east of north) of the propagation direction, and the dip angle measured from the horizontal (co-dip) of the magnetic field vector. These parameters change along the propagation path and these changes are incorporated in the WKB or mode conversion formulations.

The complex relative permittivity of the Earth, N_g, is given by:

$$N_g = \varepsilon/\varepsilon_0 - i\frac{\sigma}{\omega\varepsilon_0} \tag{28}$$

where:

σ : ground conductivity,

$\varepsilon/\varepsilon_0$: relative ground permittivity,

ε_0 : permittivity of free space,

ω : angular propagation frequency.

Table VI gives recommended values for these parameters.

TABLE VI – *Conductivity and relative permittivity of the Earth*

	Conductivity σ (S/m)	Relative permittivity ε_r
Sea water	5	80
Land	2×10^{-3}	15
Polar ice cap	2.5×10^{-5}	3

5. Results of field-strength calculation

Figures 9, 10, 11 and 12 illustrate the degree to which computed field-strength values simulate measured propagation data. These figures show the vertical electric field strength as a function of propagation distance. The ionospheric profiles listed in Tables II and III were incorporated into these field-strength computations.

Figures 9 and 10 show the comparison between fields computed assuming a horizontal homogeneous ionosphere [Pappert and Shockey, 1976] and data recorded by the US Navy [Morfitt, 1977]. These data were recorded aboard inflight aircraft at various frequencies for propagation over midlatitude sea-water paths for daytime summer conditions and for night-time winter conditions. Results using the daytime ionospheric conductivity profile with $\beta = 0.5$ km^{-1} and $H' = 70$ km are shown in Fig. 9. The results obtained using the night-time profile $\beta = 0.5$ km^{-1} and $H' = 87$ km are shown in Fig. 10.

Measurements of the Omega signal (13.6 kHz) have been made during a quiet time over a path from La Réunion (22.0 S, 56.0 E) to Inubo (35.7 N, 140.9 E). Analysis of the sunrise amplitude fading and the diurnal shift in phase and amplitude gives the following waveguide parameters:

Daytime $\beta = 0.3$ km^{-1} and $H' = 75.0$ km

Night-time $\beta = 0.5$ km^{-1} and $H' = 88.5$ km

[Kikuchi, 1986].

Experimental measurements at 45 and 60 kHz have been obtained aboard an inflight aircraft during a flight over the Greenland ice cap. These transmissions originated in England and the aircraft flight path traversed the Greenland ice cap terminating at Sondrestrom, Greenland. Comparison of these field-strength measurements to computed field-strength predictions is shown in Figs. 11 and 12. The method of calculation used to construct these figures is the mode conversion program [Pappert and Shockey, 1976].

The ground conductivity was input as 5S/m for the seawater section of the path and 2.5×10^{-5} S/m for the Greenland ice cap. The profile $\beta = 0.3$ km^{-1}, $H' = 72$ km was used as input to the calculations for simulating the measured data.

6. VLF transmission phase stability

In the Earth-ionosphere waveguide the phase of the VLF field may display short-term variations caused by the irregular nature of the boundaries of the waveguide, in addition to long-term variations associated with diurnal and seasonal changes in the ionosphere. Superimposed on these regular variations are phase changes due to ionospheric disturbances caused by solar X-ray flares, and by energetic particle precipitation into the D-region, associated with geomagnetic and auroral storms, and with solar proton events. All of these phenomena affect VLF transmission phase, and they are associated with different time and space scales [AGARD, 1982].

VLF transmission phase stability is an important parameter which must be considered for such applications as VLF navigation, frequency comparison and time synchronization. For such applications, if the user has a choice of transmission paths, as for example with the Omega navigation system, those which are dominantly single mode should be employed. When two or more modes are present, the phase stability of the total field will vary with distance in a complex oscillatory manner and will clearly be worse for some ranges of distance. The use, for example, of VLF transmissions over distances less than 1,000 km should be avoided, since it is in this distance range that the first major minimum is found. This minimum in field strength is associated with an anti-phase relation between two components, a ground- and a sky-wave of almost equal amplitude. In this distance range the diurnal variation of phase can be unpredictably asymmetrical, since the direction of rotation of the phase of the resultant depends on which component is stronger at the time [Belrose, 1968].

While multi-mode propagation is particularly severe at short distances, it can be a problem at all distances. The magnitude of the effect is a function of frequency, distance, time-of-day and ground conductivity. Phase stability is clearly worse in the vicinity of field strength minima (see Figures 9 and 10).

The regular variations of VLF phase, and the changes associated with ionospheric disturbance have been studied by many researchers, and there is a great deal of information available in the literature [Belrose, 1968; AGARD, 1982]. However, there are few statistical studies that are useful for the design of systems. Short-term variations of phase are even less well documented. Watt [1967] has summarized data available at that time, and has shown how the standard deviation of phase varies as a function of frequency (for the 10 - 20 kHz band), distance (for long paths d > 1,000 km) and time-of-day (day and night conditions). More recently Pan and Tian [1988] have published results of a study in China of 12.5 kHz phase stability for 500-3,000 km North-South paths under night-time conditions. The authors have developed a mathematical expression for the standard deviation of phase that takes into account multi-mode effects and that agrees well with this experiment.

VLF transmission phase stability is a topic that needs further study.

7. Future work

The theory of radio-wave propagation at ELF and VLF, necessary to estimate field strengths, is now becoming fairly well understood. Two competing theories are used to describe propagation in the VLF bands: the wave-hop theory and the waveguide mode theory.

The solutions obtained from the wave-hop theory (see Report 265) are generally most suitable for short distances and the higher (LF) frequencies, while the waveguide mode theory is most suitable for longer distances and the lower (VLF) frequencies. More precise mode field calculations require inclusion of transverse electric (TE) as well as transverse magnetic (TM) modes and the conversion between these types of modes. The inclusion of both mode polarizations is important for the computation of both horizontal and vertical fields between elevated transmitters and receivers.

The wave guide mode theory seems to describe better certain features of VLF propagation, e.g. the phase steps at dawn which are observed on long east-to-west transmissions, than does the ray-path wave-hop theory. The calculation of field strengths can be simpler using the waveguide mode theory than the wave-hop method for many cases. More comprehensive comparisons should be made between solutions using the waveguide mode method and wave-hop method.

It has been shown that there is limited agreement between theoretical calculations and measurement. However, further experimental observations particularly at several frequencies, between 10 and 30 kHz, over sea water and land of various conductivities, and at representative latitudes are needed. There are probably sufficient measurements of phase already available, the problem here is that the data had not been systematically analysed. The observations need to be repeated sufficiently often to demonstrate their stability. With such measurements it will be possible to determine values of the excitation factors, attenuation rates and phase velocities which in themselves could be used as a basis for calculation of field strength and phase over different paths. More importantly, however, these experimental propagation parameters should be compared with theory and, if necessary, the theory should be refined or its input parameters adjusted. It is likely that greater discrepancies will be observed for night-time than for daytime conditions.

There has been, during the last few years, a renewed interest in ELF propagation and communications (see [IEEE Journal of Oceanic Engineering, 1984], AGARD [1982] and [CCIR, 1982-86]). In particular, new (and overview) information is given on ELF propagation, on ELF noise, and on modelling the ambient and disturbed ionosphere. Comparisons are made between predicted and measured field strengths.

It should be noted that these models of the ambient and disturbed ionosphere, which are reported to provide agreement between predicted and available ELF propagation data, could also be used to predict VLF field strengths, at least by those administrations who are able to make such calculations.

A number of computer programs has been developed to calculate VLF/LF (frequencies below about 60 kHz) field strength employing the waveguide mode theory. The most complete long wave prediction capability (LWPC) is the program developed by Ferguson [1988]. It is in fact a program package, that comprises a collection of programs that have been developed by the author and his colleagues over the years [Pappert and Shockey, 1971, 1972a, 1972b and 1976; Morfitt and Shellman, 1976], that are exercised separately or in sequence depending on the application. The execution of these individual programs can be set up by a driven program which automates the process. The theoretical basis for the method is exact. The model ionosphere is, however, an approximate one which characterizes the conductivity as exponentially increasing with height (see section 4.4, Tables I and II). This two parameter model can be varied step-wise if required along the great circle path. The lower boundary of the waveguide is defined by a detailed map of the world based largely on geological formations.

More measurements are needed to establish seasonal changes [CCIR, 1986-90], and to establish differences between middle, low and high latitudes. The shadowing effect of the Greenland ice cap is important. Attenuation rates for signals propagating across the Greenland ice cap are 1.3 dB/1000 km by night and 22 dB/1000 km by day. Since daytime solar proton disturbances result in a further lowering of the ionosphereric reflecting boundary, this results in attenuation rates that are still markedly greater, to such an extent that signal reception is no longer possible. Estimates of field strength for daytime paths agree well with the observed results at middle latitudes, using $\beta = 0.3$ km^{-1} and $H' = 74$ km, providing the effects of the poorly conducting ground are properly taken into account. However, at high latitudes there may be significant dependence on seasonal and solar cycle changes in ionospheric reflectivity.

At low latitudes it is not currently possible to theoretically calculate diurnal phase and amplitude variations for transequatorial paths propagating westwards. Theoretical work is needed to derive the variation of all relevant waveguide parameters, including mode conversion. The inability to calculate corrections for westward propagating transequatorial paths is severely limiting the effectiveness of OMEGA/VLF navigation. Related to this is the need for experimental definition of the variation of VLF parameters with azimuth, latitude and frequency in the vicinity of the magnetic equator.

Research employing atmospherics as natural VLF sources on frequencies below 10 kHz is being carried out by various groups. A statistical method of analysing atmospherics in this frequency range has been developed at the Heinrich-Hertz Institute in Berlin [Volland *et al.*, 1970] which permits the determination of the location of individual thunderstorms as well as of the transmission function of the ionospheric waveguide in amplitude and phase [Frisius *et al.*, 1970; Harth, 1971]. VLF atmospherics, in spite of very limited knowledge of the source characteristics, can be used for deducing empirical conductivity profiles which are useful for long path propagation prediction conditions; the method is especially valuable for studying paths where multi-frequency transmissions are not otherwise available [Hughes *et al.*, 1974; Hughes and Pappert, 1975]. In the United States of America multi-frequency pulsed and phase coherent transmissions between 9.4 and 31.25 kHz have been used for propagation studies over very short and medium paths and over the long-distance path from Hawaii to California [Morfitt, 1971 and 1973]. Observations of VLF reflectivity for a short path near Thule, Greenland have been made during several years [Pagliarulo *et al.*, 1979]. The experimental technique utilizes 100 μsec VLF pulses radiated from a 130 metre vertical antenna [Lewis *et al.*, 1973] to deduce ionospheric reflection coefficients from 6 to 35 kHz.

A desirable way to carry out these measurements would be to use an aircraft flying along great circles between transmitters and field receiving stations. In this way the mode structure at the receivers could be determined, especially at night for paths up to 5000 to 7000 km depending on frequency. The fixed receivers which would monitor the signals continuously could then be used to determine changes in the propagation parameters resulting from diurnal seasonal variations and changes caused by differences in solar activity as well as mode conversion factors.

The other approach which is also desirable is to use measurements by rockets or ground-based techniques to determine the vertical variations of electron density in the lower ionosphere. The resulting profiles could then be used to calculate ionospheric reflection coefficients. These would then be used to calculate the VLF mode parameters for comparison with the experimental results or for direct calculation of the mode parameters. Electron density measurements are particularly required at heights below 70 km where there are large discrepancies in existing observations, at night-time and at low latitudes.

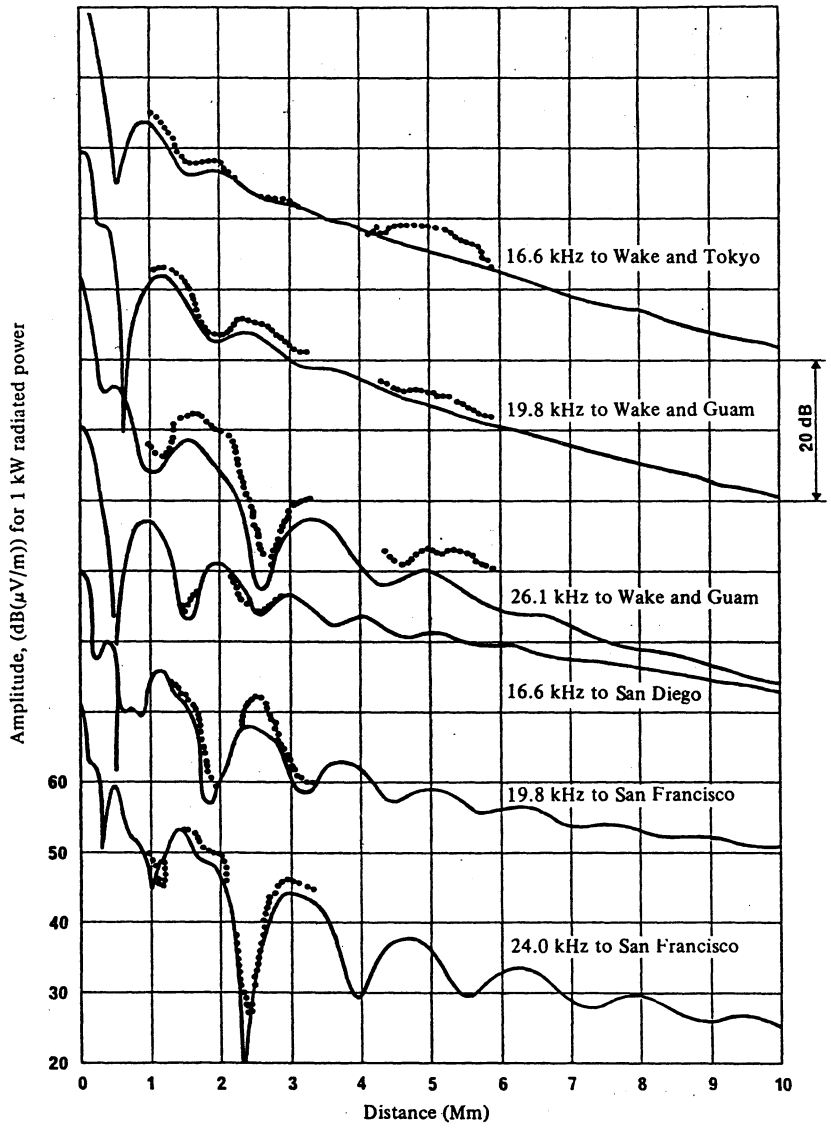

FIGURE 9 – *Propagation over the Pacific Ocean of signals transmitted from Hawaii (daytime, summer)*

——— predictions

..... observations

Note. – The amplitude scale applies to the lowest curve; the other curves are displaced by multiples of 20 dB.

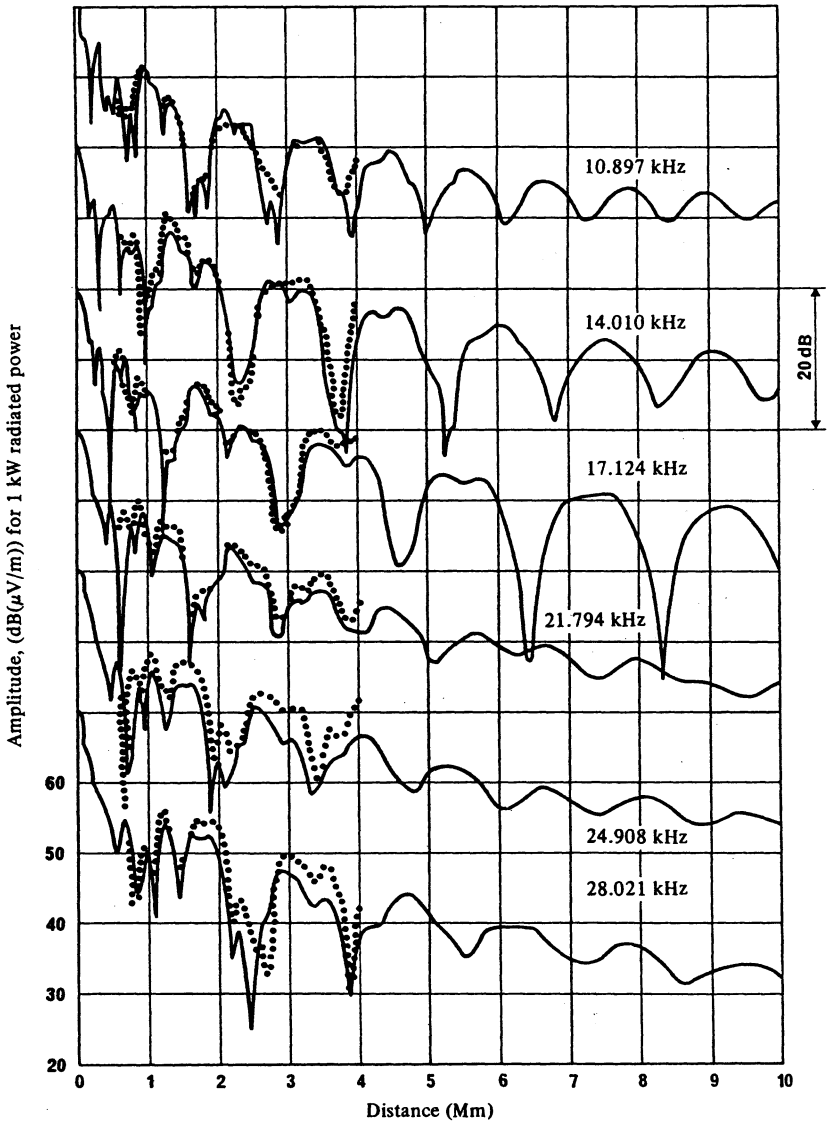

FIGURE 10 – *Propagation over the Pacific Ocean of signals transmitted from Hawaii to Southern California (night-time, winter)*

——— predictions

..... observations

Note. – The amplitude scale applies to the lowest curve; the other curves are displaced 20 dB from each other.

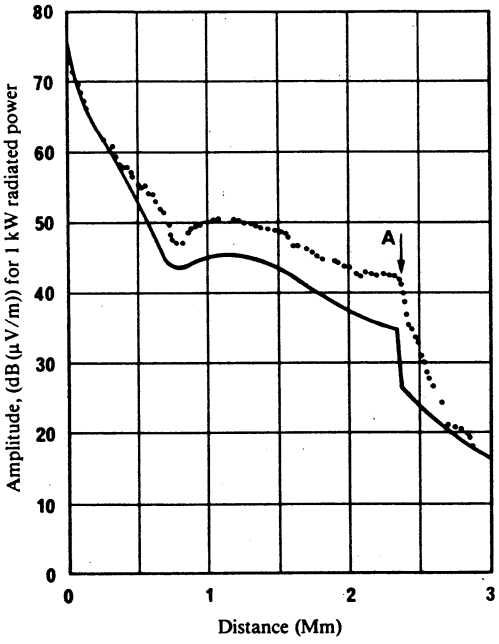

FIGURE 11 – *Daytime high latitude propagation across the Greenland ice cap (45 kHz)*

——— predictions

••••••• observations

A ice cap starts

Preston, U.K. to Sondrestrom (Greenland)
Frequency: 45 kHz
$\beta = 0.3\ km^{-1}$, $H' = 72$ km

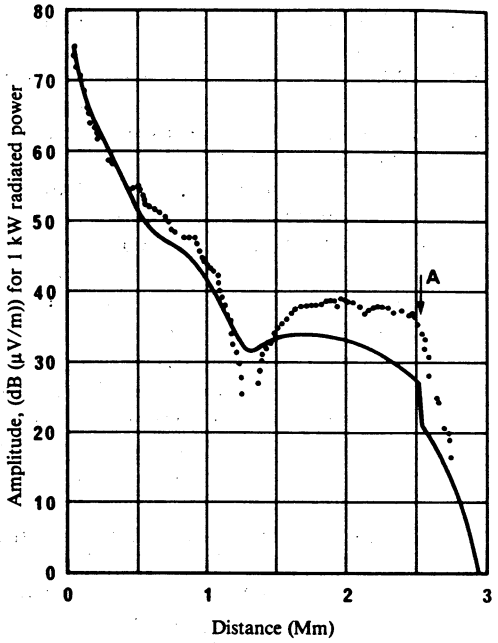

FIGURE 12 – *Daytime high latitude propagation across the Greenland ice cap (60 kHz)*

——— predictions

••••••• observations

A ice cap starts

Rugby, U.K. to Sondrestrom (Greenland)
Frequency: 60 kHz
$\beta = 0.3\ km^{-1}$, $H' = 72$ km

REFERENCES

AGARD [1982] Ed. J. S. Belrose, *Medium, Long and Very Long Wave Propagation (at frequencies less than 3000 kHz).* Conf. Proc. No. 305, NASA Accession No. N82-27613. National Technical Information Service, Springfield, VA 22161, USA.

AL'PERT Ya. L., GUSEVA, E. G. and FLIGEL, D. S. [1967] Propagation of LF electro-magnetic waveguide. Academy of Sciences of the U.S.S.R.

ARAKI, T. [1973] Anomalous diurnal changes of transequatorial VLF radio waves. *J. Atmos. Terr. Phys.*, Vol. 35, 4, 693-703.

BANNISTER, P. R. [1979] Summary of extremely low frequency (ELF) field strength measurements made in Connecticut during 1975. *Radio Sci.*, Vol. 14, 1, 103-108.

BARR, R. [1971a] The propagation of ELF and VLF radio waves beneath an inhomogeneous anisotropic ionosphere. *J. Atmos. Terr. Phys.*, Vol. 33, 343-353.

BARR, R. [1971b] The effect of the earth's magnetic field on the propagation of ELF and VLF radio waves. *J. Atmos. Terr. Phys.*, Vol. 33, 1577-1583.

BELROSE, J.S. [1968] - Low and very low frequency radio propagation. AGARD lecture series XXIX, NTIS Acces. No. AD 676788, National Technical Information Service, VA, 22161, United States.

BEUKERS, J. M. [1973] Accuracy limitations of the OMEGA navigation system employed in differential mode. *J. Inst. Nav.*, Vol. 20, 1, 81-92.

BEUKERS, J. M. [1974] A review and application of VLF and LF transmissions for navigation and tracking. *J. Inst. Nav.*, Vol. 21, 2, 117-133.

BICKEL, J. E. [1967] VLF attenuation rates deduced from aircraft observations near the antipode of NPM. *Radio Sci.*, Vol. 2, (New Series), 575-580.

BICKEL, J. E., FERGUSON, J. A. and STANLEY, G. V. [1970] Experimental observations of magnetic field effects on VLF propagation at night. *Radio Sci.*, Vol. 5, 19-25.

BLAIR, B. E. CROW, E. L. and MORGAN, A. H. [1967] Five years of VLF world-wide comparison of atomic frequency standards. *Radio Sci.*, Vol. 2, (New Series), 627-636.

BUDDEN, K. G., [1955] The numerical solution of differential equations governing reflection of long radio waves from the ionosphere. *Proc. Roy. Soc.* A227, 516-537.

BUDDEN, K. G. [1961] The waveguide-mode theory of wave propagation. Prentice Hall Inc., Englewood Cliffs, NJ, USA.

BURGESS, B. [1970] VLF phase delay variability and design of long range navigation aids. *Phase and Frequency Stabilities in Electromagnetic Wave Propagation*. Ed. K. Davies, Technivision, Slough, United Kingdom.

BURROWS, M. L. [1978] *ELF Communications Antennas.* Peter Peregrinus Ltd., Stevenage, England.

BURROWS, M. L. and NIELSSEN, C. W. [1972] ELF communication system design. IEEE International Conference on Engineering in the Ocean Environment, 95-107.

CASSELMAN, C. J., HERITAGE, D. P. and TIBBALS, M. L. [1959] VLF propagation measurements for the Radux-Omega navigation system. *Proc. IRE*, 47, 829-839.

CHAPMAN, F. W., LLANWYN JONES, D., TODD, J. D. W. and CHALLINOR, R. A. [1966] Observations on the propagation constant of the earth-ionosphere waveguide in the frequency band 8 c/s to 16 kc/s. *Radio Sci.*, Vol. 1, 1273-1282.

CHILTON, C. J., CRARY, J. H. and CROMBIE, D. D. [1969] A comparison of middle and low latitude sunrise VLF fading observed on the 1967 voyage of the Oceanographer. Proc. Third International Symposium on Equatorial Aeronomy, Ahmedabad, India, February 3-8, Vol. 1 105-113.

COMPUTATION LABORATORY AT CAMBRIDGE [1945] *Tables of the Modified Hankel Functions of Order One-Third and of their Derivatives.* Harvard University Press, Cambridge, Ma., USA.

CROMBIE, D. D. [1964] Periodic fading of VLF signals received over long paths during sunrise and sunset. *NBS J. Res.*, Vol. 68D, 27-34.

CROMBIE, D. D. [1966] Further observations of sunrise and sunset fading of VLF signals. *Radio Sci.*, Vol. 1, (New Series), 47-51.

CROMBIE, D. D. [1967] The waveguide mode propagation of VLF radio waves to great distances. IEE (London) Conf. Publ., 36.

CROMBIE, D. D., ALLAN, A. H. and NEWMAN, M. [1958] Phase variations of 16 kHz transmissions from Rugby, observed in New Zealand. *Proc. IEE*, Vol. 105B, 301-304.

DAVIS, J. R. [1976] Localized nighttime D-region disturbances and ELF propagation. *J. Atmos. Terr. Phys.*, Vol. 38, 1309-1317.

DAVIS, R. M. and BERRY, L. A. [1977] A revised model for the electron density in the lower ionosphere. Command and Control Technical Center (DCA), Tech. Rep. 111077, NTIS Accession No. AD17883. National Technical Information Service, Springfield, Va. 22161, USA.

FERGUSON, J. A. [1980] Ionospheric profiles for predicting nighttime VLF/LF propagation. NOSC TR 530, NTIS Accession No. ADA 085399. National Technical Information Service, Springfield, Va. 22161, USA.

FERGUSON, J.A. [1988] - Status of the naval ocean systems long wave propagation capability "LWPC". Paper presented at Third Workshop on ELF/VLF Radio Noise, Stanford University.

FOLEY, G., WAND, I. C. and JONES, T. B. [1973] Studies of the modal parameters of VLF radio waves propagated below the night-time ionosphere. *J. Atmos. Terr. Phys.*, Vol. 35, 2111-2122.

FRISIUS, J., HEYDT, G. and HARTH, W. [1970] Observations of parameters characterising the VLF atmospherics activity as a function of the Azimuth. *J. Atmos. Terr. Phys.*, Vol. 32, 1403-1422.

GALEJS, J. [1967a] Propagation of VLF waves below an anisotropic stratified ionosphere with a transverse static magnetic field. *Radio Sci.*, Vol. 2, (New Series), 557-574.

GALEJS, J. [1967b] Propagation of VLF waves below anisotropic ionosphere models with a dipping static magnetic field. *Radio Sci.*, Vol. 2 (New Series), 1497-1512.

GALEJS, J. [1972] *Terrestiral Propagation of Long Electromagnetic Waves.* Pergamon Press, New York/Oxford.

GALLENBERGER, R. and SWANSON, E. [1971] Variations in Omega propagation parameters. NELC/TR 1773. Naval Electronics Laboratory Center, San Diego, Calif., USA.

HARTH, W. [1971] Sudden anomalies of spectral atmospherics parameters during SID's. Proc. VLF Symposium, Ødo-Sandefjord, Norway.

HUGHES, H. G. [1971] Differences between pulse trains of ELF atmospherics at widely separated locations. *J. Geophys. Res.*, Vol. 76, 2116-2125.

HUGHES, H. G. and GALLENBERGER, R. J. [1974] Propagation of extremely low-frequency (ELF) atmospherics over a mixed day-night path. *J. Atmos. Terr. Phys.*, Vol. 36, 1643-1661.

HUGHES, H. G., GALLENBERGER, R. J. and PAPPERT, R. A. [1974] Evaluation of night-time exponential ionospheric models using VLF atmospherics. *Radio Sci.*, Vol. 9, 1109-1116.

HUGHES, H. G. and PAPPERT, R.A. [1975] Propagation prediction model selection using VLF atmospherics. *Geophys. Res. Lett.*, Vol. 2, 96-98.

HUGHES, H. G. and THEISSEN, J. F. [1970] Diurnal variations in the apparent attenuations of ELF atmospherics over two different propagation paths. *J. Geophys. Res.*, Vol. 75, 2795-2801.

IEEE JOURNAL OF OCEANIC ENGINEERING [July, 1984] Special Issue on ELF communications. Vol. OE-9.

JOHLER, J. R. and LEWIS, R. L. [1969] Extra-low frequency terrestrial radio-wave field calculations with the zonal harmonic series. *J. Geophys. Res.*, Vol. 74, 2459-2470.

KAISER, A. B. [1969] An explanation of VLF diurnal phase change observations. *Radio Sci.*, Vol. 4, 17-21.

KIKUCHI, T. [1983] Anomalous diurnal phase shifts of Omega VLF waves (10-14 kHz) on the east-west low latitude and transequatorial paths. *J. Atmos. Terr. Phys.*, Vol. 45, 743-751.

KIKUCHI, T. [1986] Waveguide model analyses of Omega VLF wave propagation at 13.6 kHz. J. Atmos. Terr. Phys., 48, 15-23 .

KIKUCHI, T. and OHTANI, A. [1984] Anomalous interference in Omega VLF wave propagation on east-to-west equatorial paths. *J. Atmos. Terr. Phys.*, Vol. 46, 697-703.

KUHNLE, P. F. and SMITH, R. D. [1964] Rome Air Development Center. Tech. Rep. RADC-TR-64-360, NTIS Accession No. ADAOC1701. National Technical Information Service, Springfield, Va. 22161, USA.

LEWIS, R. L. and JOHLER, J. R. [1976] Correction of numerical results in "ELF terrestrial radio wave field calculations with the zonal harmonic series". *Radio Sci.*, Vol. 11, 75-81.

LEWIS, E. A, RASMUSSEN, J. E., and KOSSEY, P. A. [1973] Measurements of ionospheric reflectivity from 6 to 35 kHz. *J. Geophys. Res.*, Vol. 78, 19, 3903-3912.

LYNN, K. J. W. [1967] Anomalous sunrise effects observed on a long trans-equatorial VLF propagation path. *Radio Sci.*, Vol. 2 (New Series), 521-530.

LYNN, K. J. W. [1969] Multisite observations of the VLF transequatorial propagation anomaly. *Radio Sci.*, Vol. 4, 203-211.

LYNN, K. J. W. [1973] VLF mode conversion observed at middle latitudes. *J. Atmos. Terr. Phys.*, Vol. 35, 439-452.

LYNN, K. J. W. [1975] The transequatorial reception of Omega (13.6 kHz) transmissions. *J. Atmos. Terr. Phys.*, Vol. 37, 1395-1399.

LYNN, K. J. W. [1977] VLF modal interference over west-east paths. *J. Atmos. Terr. Phys.*, Vol. 39, 347-357.

LYNN, K. J. W. [1978] Some differences in diurnal phase and amplitude variations for VLF signals. *J. Atmos. Terr. Phys.*, Vol. 40, 145-150.

MAHMOUD, S. F. and BEAL, J. C. [1971] VLF propagation parameters derived from observations of sunrise and sunset phenomena. *Proc. IEE*, Vol. 118, 1351-1357.

MEARA, L. A. [1973] VLF modal interference effects observed on transequatorial paths. *J. Atmos. Terr. Phys.*, Vol. 35, 305-315.

MORFITT, D. G. [1971] Analysis of a multimode propagation concept for predicting VLF signal strengths at night. Naval Electronics Laboratory Center Tech. Rep. TR 1798, NTIS Accession No. AD738846. National Technical Information Service, Springfield, Va. 22161, USA.

MORFITT, D. G. [1973] Computer techniques for fitting electron density profiles to oblique-path VLF propagation data. Naval Electronics Laboratory Center Tech. Rep. TR 1854, NTIS, Accession No. AD757341. National Technical Information Service Springfield, Va. 22161, USA.

MORFITT, D. G. [1977] Effective electron density distributions which describe VLF/LF propagation data. Naval Ocean Systems Center Tech. Rep. TR141, NTIS, Accession No. ADA047508. National Technical Information Service Springfield, Va. 22161, USA.

MORFITT, D. G. and SHELLMAN, C. H. [1976] MODESRCH, an improved computer program for obtaining ELF/VLF/LF mode constants. Naval Electronics Laboratory Centre Interim Rep. 771, NTIS Accession No. ADA032573. National Technical Information Service Springfield, Va. 22161, USA.

NARD, G. [1972] Results of recent experiments with differential OMEGA. *J. Inst. Nav.*, 19, 2.

PAGLIARULO, R. P., TURTLE, J. P., RASMUSSEN, J. E., COOLEY, R. L. and KLEMETTI, W. I. [1979] VLF/LF reflectivity of the polar ionosphere – September 1978 to 5 May 1979. Reports RADC-TR-79-178 and 273. Rome Air Development Center, Griffiss Air Force Base, NY, USA.

PAN WEIYAN and TIAN YUSHU [1988] - Multi-mode interference and phase stability of VLF wave propagation. Proc. 1988 International Symposium on Radio Propagation (ISRP '88), Beijing, China, 40-44.

PAPPERT, R. A [1968] A numerical study of VLF mode structure and polarization below an anisotropic ionosphere. *Radio Sci.*, Vol. 3, (New Series), 219-233.

PAPPERT, R. A. [1970] Effects of elevation and ground conductivity on horizontal dipole excitation of the earth-ionosphere waveguide. *Radio Sci.*, Vol. 5, 579-590.

PAPPERT, R. A. and BICKEL, J. E. [1970] Vertical and horizontal VLF fields excited by dipoles of arbitrary orientation and elevation. *Radio Sci.*, Vol. 5, 1445-1452.

PAPPERT, R. A., GOSSARD, E. E. and ROTHMULLER, I. J. [1967] A numerical investigation of classical approximations used in VLF propagation. *Radio Sci.*, Vol. 2, 387-400.

PAPPERT, R. A. and MOLER, W. F. [1974] Propagation theory and calculations at lower extremely low frequencies (ELF). *IEEE Trans. Comm.* Vol. COM-22, 438-451.

PAPPERT, R. A. and MORFITT, D. G. [1975] Theoretical and experimental sunrise mode conversion results at VLF. *Radio Sci.*, Vol. 10, 537-546.

PAPPERT, R. A. and SHOCKEY, L. R. [1971] WKB Mode summing program for VLF/LF antennae of arbitrary length, shape and elevation. Naval Electronics Laboratory Center Interim Rep. 713, NTIS Accession No. AD728414. National Technical Information Service, Springfield, Va. 22161, USA.

PAPPERT, R. A. and SHOCKEY, L. R. [1972a] Mode conversion program for an inhomogeneous anisotropic ionosphere. Naval Electronics Laboratory Center Interim Rep. 722, NTIS Accession No. AD743948. National Technical Information Service, Springfield, Va. 22161, USA.

PAPPERT, R. A. and SHOCKEY, L. R. [1972b] WKB fields program for lower ELF. Naval Electronics Laboratory Center Interim Rep. 731, NTIS Accession No. AD757080. National Technical Information Service, Springfield, Va. 22161, USA.

PAPPERT, R. A. and SHOCKEY, L. R. [1976] Simplified VLF/LF mode conversion program with allowance for elevated, arbitrarily oriented electric dipole anennae. Naval Electronics Laborartory Center Interim Rep. 771, NTIS Accession No. ADA033412, National Technical Information Service, Springfield, Va. 22161, USA.

PAPPERT, R. A. and SMITH, R. R. [1972] Orthogonality of VLF height gains in the earth ionosphere waveguide. *Radio Sci.*, Vol. 7, 275-278.

PAPPERT, R. A. and SNYDER, F. P. [1972] Some results of a mode-conversion programme for VLF. *Radio Sci.*, Vol. 7, 913-923.

RAWLES, A. T. and BURGESS, B. [1967] Results of the two-frequency VLF transmission experiments from Criggion GBZ. *Radio Sci.*, Vol. 2, 1295-1301.

REDER, F. [1979] Propagation effects on Omega signals and methods of reducing them. Fourth Annual Meeting of the International Omega Association, San Diego, 10-12 September, Calif., USA.

RHOADS, F. J. and GARNER, W. E. [1967] An investigation of the modal interference of VLF radio waves. *Radio Sci.*, Vol. 2 (New Series), 539-546.

RINNERT, K. [1973] Electron density profiles in the lower ionosphere deduced from long path VLF wave propagation. *Radio Sci.*, Vol. 8, 829-836.

RUGG, D. E. [1967] Theoretical investigation of the diurnal phase and amplitude variations of VLF signals. *Radio Sci.*, Vol. 2, 551-556.

SHEDDY, C. H. [1968] A general analytic solution for reflection from a sharply bounded anisotropic ionosphere. *Radio Sci.*, Vol. 3, **8**, 792-795.

SNYDER, F. P. and PAPPERT, R. A. [1969] A parametric study of VLF transequatorial propagation anomaly. *Radio Sci.*, Vol. 4, 213-226.

STEELE, F. K. and CROMBIE, D. D. [1967] Frequency dependence of VLF fading at sunrise. *Radio Sci.*, Vol. 2, (New Series), 547-549.

SUZUKI, K., BABA, K., YOSHIOKA, T. and KINOSHITA, M. [1973] Phase variation and amplitude fading of NWC – 22.3 kHz signal at dawn. *J. Geomag. Geoelect.*, Vol. 25, 403-413.

TAYLOR, W. L. and SAO, K. [1970] ELF attenuation rates and phase velocities observed from slow-tail components of atmospherics. *Radio Sci.*, Vol. 5, 1453-1460.

VOLLAND, H. [1966] Die Ausbreitung langer Wellen (propagation of long waves). *Veröffentlichungen des NKGG der DDR, Reihe 11*, Vol. 2, 3-126.

VOLLAND, H., HEYDT, G. and HARTH, W. [1970] Statistical measurement of the spectral amplitude and phase of atmospherics in the VLF range. *Phase and Frequency Stabilities in Electromagnetic Wave Propagation.* Ed. K. Davies, Technivision, Slough, UK.

WAIT, J. R. [1962] *Electromagnetic Waves in Stratified Media.* Pergamon Press, New York, NY, USA.

WAIT, J. R. [1964] Two dimensional treatment of mode theory of the propagation of VLF radio waves. *NBS J. Res.*, Vol. 68D, 81-93.

WAIT, J. R. [1968a] Mode conversion and refraction in the earth-ionosphere wave-guide for VLF radio waves. *J. Geophys. Res.*, Vol. 73, 3535-3548.

WAIT, J. R. [1968b] On the theory of VLF propagation for a step model of the nonuniform earth-ionosphere wave-guide. *Can. J. Phys.*, Vol. 46, 1979-1983.

WAIT, J. R. [1970] Factorization method applied to electromagnetic wave propagation in a curved wave-guide with nonuniform walls. *Radio Sci.*, Vol. 5, 1059-1068.

WAIT, J. R. (Ed.) [1974] Special issue on extremely low frequency (ELF) communications. *IEEE Trans. Comm.*, Vol. COM-22, **4**.

WAIT, J. R. [1977] Propagation of ELF electromagnetic waves and project SANGUINE/SEAFARER. *IEEE J. Ocean. Eng.*, Vol. OE-2, **2**, 161-171.

WAIT, J. R. and SPIES, K. P. [1965] Influence of finite ground conductivity on the propagation of VLF radio waves. *NBS J. Res.*, Vol. 69D, 1359-1373.

WAIT, J. R. and SPIES, K. P. [1968] On the calculation of mode conversion at a graded height change in the earth-ionosphere wave-guide at VLF. *Radio Sci.*, Vol. 3, 787-791.

WALKER, D. [1965] Phase steps and amplitude fading of VLF signals at dawn and dusk. *NBS J. Res.*, Vol. 69D, 1435-1443.

WATT, A. D. [1967] *VLF Radio Engineering.* Pergamon Press, New York, NY, USA.

WESTERLUND, S. and REDER, F. H. [1973] VLF radio signals propagating over the Greenland ice-sheet. *J. Atmos. Terr. Phys.*, Vol. 35, 1475-1491.

WESTERLUND, S., REDER, F. H. and ABOM, C. [1969] Effects of polar cap absorption events on VLF transmissions. *Planet. Space Sci.*, Vol. 17, 1329-1374.

WILLIM, D. K. [1974] Sanguine, *ELF-VLF Radiowave Propagation*, 251-261. D. Reidel Publishing Co., Dordrecht, Netherlands.

CCIR Documents

[1982-86]: 6/228 (IWP 6/5).

[1986-1990]: 6/242 (Interim Working Party 6/5).

BIBLIOGRAPHY

CCIR Documents

[1978-82]: 6/242 (IWP 6/5).